

Transport Spectroscopy of a Coulomb Island in the Quantum Hall Regime

P. L. McEuen, E. B. Foxman, U. Meirav,^(a) M. A. Kastner, Yigal Meir, and Ned S. Wingreen
Department of Physics, Massachusetts Institute of Technology, Cambridge, Massachusetts 02139

S. J. Wind

IBM Thomas J. Watson Research Center, Yorktown Heights, New York 10598

(Received 30 January 1991)

Transport measurements of a Coulomb island, a semiconductor dot small enough that Coulomb interactions dominate transport, are presented. At moderate magnetic fields ($B=2-4$ T) the amplitude and position of the Coulomb-regulated conductance peaks show distinct periodic structure as a function of B . This structure is shown to result from the B dependence of the quantized single-particle energy states on the island. Analysis of successive peaks is used to map out the single-particle level spectrum of the island as a function of B .

PACS numbers: 73.20.Dx, 72.20.My, 73.40.Gk

Transport through nanometer-scale electron gases such as small metal particles¹ or lithographically patterned semiconductor dots² is currently a subject of great experimental and theoretical interest. In these structures the quantization of the charge and energy of the electron gas has important implications for transport. Charge quantization is important since it means that adding an extra electron to the dot can require a finite charging energy. Transport is suppressed if this charging energy exceeds $k_B T$, creating a "Coulomb island"—a small electron gas electrically isolated from the leads by Coulomb interactions. This suppression is lifted whenever the charge fluctuations required for transport do not change the total energy of the system, and a peak in the conductance results. A semiclassical stochastic model of these devices, called the Coulomb-blockade model,¹ has been remarkably successful in explaining experiments on small metal structures. Although also capable of explaining some aspects of experiments on semiconductor dots,^{3,4} this model is inappropriate at low temperatures since it ignores the quantization of the dot's energy spectrum. The discrete spectrum of dots, which has been explored by various spectroscopic techniques,⁵⁻⁷ causes such transport effects as Aharonov-Bohm-type oscillations⁷ and resonant tunneling.^{6,7}

While charge and energy quantization effects are, taken separately, well understood, the regime in which both are important is only beginning to be explored. Recent theoretical work⁸⁻¹¹ has predicted that the properties of the Coulomb-blockade conductance peaks are affected by the single-particle electronic eigenstates of the dot. In this Letter, we present an experimental study of a semiconductor dot in the quantum Hall regime, where the properties of the single-particle states are well known.^{12,13} We find that the conductance peaks reflect the properties of the quantized energy levels of the island in surprising and dramatic ways. We further show that these measurements allow spectroscopy of *all* energy levels of the island—including levels through which negli-

ble current flows.

The geometry of the device used here is shown schematically in Fig. 1(a); a detailed description may be found in Refs. 3 and 14. Briefly, it is an inverted GaAs/AlGaAs heterostructure in which electrostatic gates are used to confine and adjust the density of a two-dimensional electron gas. A negative bias applied to a lithographically patterned split upper gate defines the island¹⁵ while a positive bias applied to a lower gate ad-

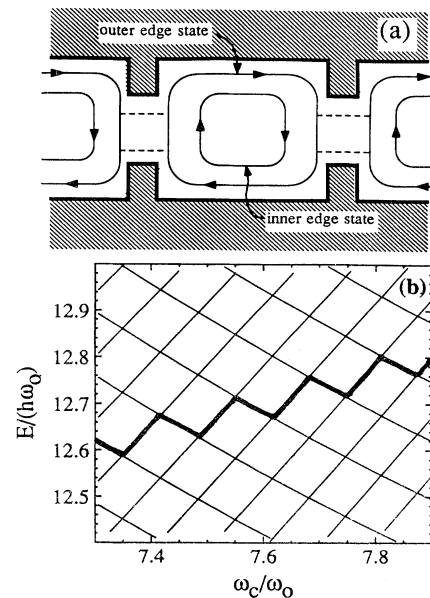


FIG. 1. (a) Schematic top view of the device, showing the path of the edge states associated with the lowest two Landau levels (LLs). The upper gate (shaded) defines a dot whose lithographic dimensions are 500 nm by 700 nm. (b) Energy levels of a dot with a parabolic confining potential $\frac{1}{2} m^* \omega_0^2 r^2$ as a function of $\omega_c = eB/m^*$ in a parameter range where two LLs are present (Ref. 12). The heavy line represents the energy of the single-particle state that is 78th lowest in energy.

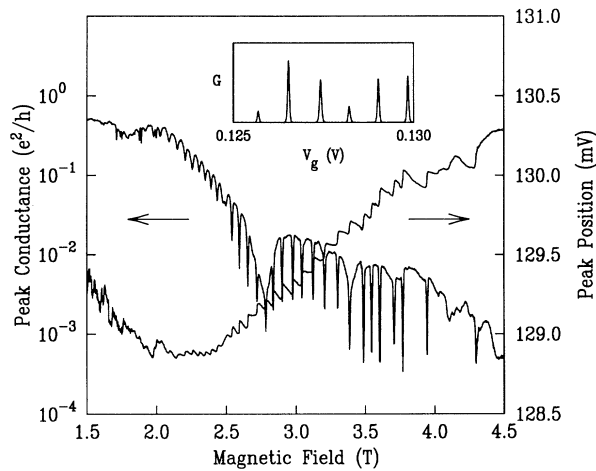


FIG. 2. Height and position of a conductance peak as a function of magnetic field at base temperature. The temperature of the electron gas is approximately 0.1 K (Ref. 3). Inset: Conductance vs V_g for the device at $B=3$ T. Full scale is $0.03e^2/h$.

justs the electron density. The conductance G versus gate voltage V_g applied to the lower gate is shown in the inset of Fig. 2. As reported previously,³ the conductance consists of a periodic series of sharp peaks.

We have studied, in detail, the dependence of the amplitude and position of these conductance peaks on magnetic field B . At low fields ($B < 1$ T), the amplitude shows strong random fluctuations with B which give way to more systematic behavior at higher magnetic fields. Figure 2 shows the position and amplitude of a particular conductance peak for $B=1.5$ – 4.5 T. At roughly periodic values of B , the peak amplitude drops by as much as an *order of magnitude*. Commensurate with these dips, oscillations are observed in the position of the peak. This structure washes out rapidly with increasing temperature and is almost entirely destroyed by $T \sim 0.3$ K [Figs. 3(a) and 3(b)], although the peaks in the conductance versus gate voltage remain well defined.

We now discuss the origin of this behavior. The basic periodicity of the series of conductance peaks shown in the inset of Fig. 2 can be understood within the standard Coulomb-blockade model.^{1,4} A valley corresponds to a gate voltage where an integer number of electrons minimizes the electrostatic energy of the dot. Changing the occupancy of the dot requires a finite charging energy, and transport is suppressed. A conductance peak, on the other hand, corresponds to a gate voltage where a half-integer charge $(N - \frac{1}{2})e$ on the dot would minimize the electrostatic energy. Since the actual charge on the dot is restricted to integer values of e , it fluctuates between $(N-1)e$ and Ne with no cost in charging energy, and transport can occur at $T=0$. The spacing of the peaks is determined by the gate-voltage change required to change the occupancy of the dot by one electron.

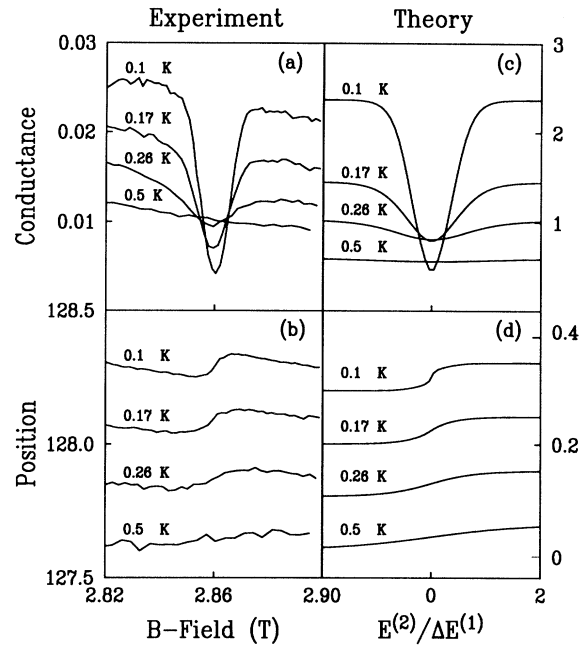


FIG. 3. Temperature dependence of (a) the peak amplitude in e^2/h and (b) the peak position in mV of a peak over a narrow B range containing one dip. Also shown are the predictions of the three-level model described in the text for (c) the peak amplitude in units of $(e^2/h)\Gamma^{(1)}/\Delta E^{(1)}$ and (d) the peak position in meV, both for $\Delta E^{(1)}=0.05$ meV. All but the lowest peak-position curves have been offset for clarity.

If $k_B T$ is less than the single-particle level spacing, the discreteness of the energy levels of the dot must be considered, since in this case the charge fluctuation between $(N-1)e$ and Ne involves emptying and filling the N th single-particle state in the dot. The energy E_N of this single-particle state directly affects the position of the peak. For example, if E_N increases, the peak occurs at a higher V_g since, roughly speaking, the state is more difficult to fill. Elementary arguments show that, for constant Coulomb energy U , the position of the N th conductance peak at $T=0$ can be written as^{1,4,10}

$$V_g(N) = (1/ae)[(N - \frac{1}{2})U + (E_N - \mu)] + \text{const},$$

where μ is the chemical potential in the leads and a is a dimensionless constant relating changes in gate voltage to changes in the electrical potential of the dot. The constant a can be determined from the temperature dependence of the width of a conductance peak³ and is found to be 0.4 for this device.¹⁶

The position of the N th conductance peak is thus determined by a Coulomb term proportional to $(N - \frac{1}{2})U$ and by a single-particle term proportional to $E_N - \mu$. In our device, the dominant term is the Coulomb term, producing conductance peaks roughly periodic in V_g . The Coulomb energy does not vary with magnetic field, however, so the variation of the position of the peak

shown in Fig. 2 results from variations in E_N .

To understand why E_N exhibits a periodic modulation, consider Fig. 1(b), a plot of the single-particle energy-level spectrum of a dot in a high magnetic field. In the parameter range shown, the spectrum consists of two Landau levels (LLs), which, in turn, are composed of discrete nondegenerate states because of the confinement potential^{12,13} (spin is suppressed for clarity). States in the first LL fall in energy with increasing B while those in the second LL rise. The thick line in Fig. 1(b) shows the behavior of E_N , the state occupied by the N th electron on the dot, as a function of B . This electron alternately occupies a state in the first LL and a state in the second LL as the magnetic field is increased. Consequently, the position of the N th peak oscillates, as is evident in the data of Fig. 2.

These oscillations will be clear if there are two Landau levels occupied. With many more than two, the simple oscillations give way to complicated fluctuations, while with less than two there are no oscillations because all the electrons are in the lowest LL.¹⁰ In Fig. 2, the oscillations become clear around $B=2$ T, and then die out around $B=4$ T. We thus attribute these field values to filling factors of $\nu=4$ and $\nu=2$, respectively. In addition, the oscillations change character above a B value (2.5 T) that roughly corresponds to $\nu=3$. In this regime, the second LL is likely spin polarized due to the enhancement of the g factor.¹⁷ We note that each oscillation in Fig. 2 represents the transfer of one electron from the second LL to the first LL. We are thus watching the magnetic depopulation of the second LL, *one electron at a time*.

We now consider the behavior of the amplitude of a conductance peak. The behavior evident in Figs. 2 and 3 follows if (a) only two LLs are occupied, and (b) the states of the second LL do not couple to the leads.^{7,18} These assumptions are schematically illustrated in Fig. 1(a). At a particular B , if the N th single-particle state is in the first LL [the outer-edge state shown in Fig. 1(a)], it couples well to the leads and transport can occur by resonant tunneling through this state. If the N th state is in the second LL [the inner-edge state in Fig. 1(a)], however, the peak amplitude is suppressed since the coupling to this state is minimal. A dip in amplitude is thus expected whenever the N th state is in the second LL, i.e., when the position of the peak is moving up in energy.¹⁹ This is indeed what is observed in Fig. 2. The dip in conductance disappears when $k_B T$ becomes comparable to the single-particle level spacing in the first LL, since transport can then occur by thermal activation to the nearest energy state in the first LL.

The arguments above can be made quantitative using the theory of Meir, Wingreen, and Lee.¹¹ This theory gives an explicit expression for the conductance in terms of the interaction energy U , the single-particle energies E_i , and the single-particle elastic-tunneling widths Γ_i . The main features of the experimental data can be ac-

counted for by a simple three-level model: two states (representing states in the first LL) with energy separation $\Delta E^{(1)}$ and equal elastic widths $\Gamma^{(1)}$ and a single state (representing a state in the second LL) with an energy $E^{(2)}$ that increases with B and has negligible coupling to the leads ($\Gamma^{(2)}=0$). In Fig. 3, the temperature dependence of the height and position of a particular conductance peak are compared with the theoretical predictions for the three-level system. The agreement between theory and experiment is excellent,²⁰ considering that the only free parameter determining the shape of the theoretical curves is the energy-level spacing in the first LL, $\Delta E^{(1)}$. This spacing is found to be 0.05 meV for this peak at this magnetic-field value. Further, the elastic width can be obtained from the height of the conductance peak and is found to be $\Gamma^{(1)}=0.0006$ meV, assuming symmetric barriers. The theory also predicts a significant broadening of the width of the conductance peak at the dip in amplitude, which is also observed (not shown).

Having understood the behavior of a single conductance peak, we now turn our attention to the behavior of successive peaks, as shown in Fig. 4(a). As indicated by the arrows, a single-particle level within a given LL moves continuously through successive conductance peaks, allowing it to be tracked over a wide range of magnetic field.¹⁹ The Coulomb portion U/ae of the peak separation in Fig. 4(a) is approximately constant and

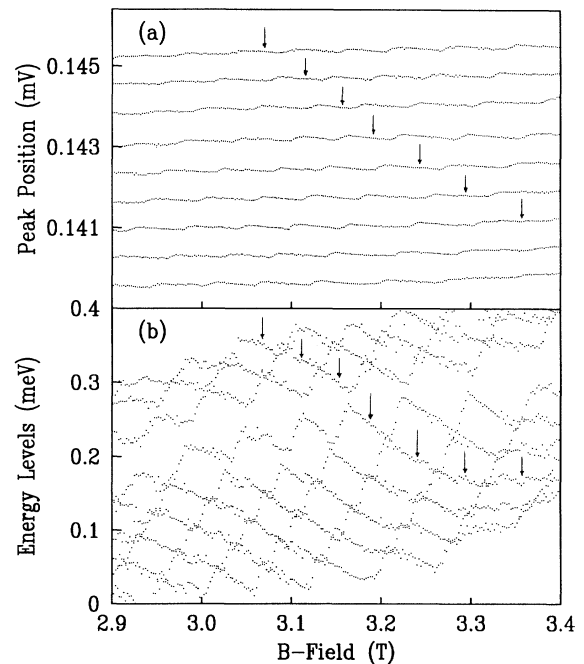


FIG. 4. (a) Peak position vs B for a series of consecutive conductance peaks. The arrow follows a particular state in the first LL as it moves through successive peaks. (b) Single-particle energy-level spectrum inferred from (a) as described in the text. The zero of the energy scale is arbitrary.

can be removed by subtracting a constant gate-voltage spacing (chosen to be 0.685 mV) between successive peaks. Furthermore, the resulting peak positions in V_g can be converted to energies using the factor $\alpha=0.4$ determined from the temperature dependence of the width of a conductance peak.³ Doing this, we obtain the results shown in Fig. 4(b). This plot represents the *single-particle energy-level spectrum of the island* as a function of B .

The level spectrum of Fig. 4(b) is qualitatively very similar to the theoretical spectrum shown in Fig. 1(b). The curves moving to higher (lower) energy with B are states in the second (first) LL.¹⁹ The parts of the curves inferred from different conductance peaks match up well, indicating that the assumption of a constant Coulomb term is a reasonably good one. There are deviations, however, such as the discontinuity in the inferred single-particle states starting near 0.2 meV. Other regions of magnetic field show even more unusual behavior. These deviations indicate the importance of interaction effects beyond the scope of the constant-Coulomb-energy model and will be explored in future experiments.

The quantitative aspects of Fig. 4(b) are also in excellent agreement with expectations. For example, the increase in energy of the states in the second LL relative to those in the first LL with increasing B is approximately 3.6 meV/T. This value compares favorably with theoretical predictions for parabolic confinement¹² ($\sim 2\hbar\omega_c/B = 3.2$ meV/T) or hard-wall confinement¹³ ($\sim 3\hbar\omega_c/B = 4.8$ meV/T) when the second LL is nearly depopulated. The single-particle energy-level spacings within a LL can be found directly from Fig. 4(b); they are $\Delta E^{(1)} = 0.05$ meV and $\Delta E^{(2)} = 0.1$ meV. The level splitting $\Delta E^{(1)}$ inferred in this way agrees with the value of $\Delta E^{(1)} = 0.05$ meV obtained earlier from the temperature dependence of a peak dip.

The level splitting in the second LL is about twice that in the first LL, again suggesting that the second LL is spin resolved at this field value (and hence has half as many states per unit energy). The periodic spacing of the states in the first LL is somewhat unexpected, since spin splitting would in general group the states into twos. We note, however, that the anticipated bare spin splitting $g\mu_B H = 0.06$ meV at 3 T, and so the observation of a single energy spacing may simply be because the spin splitting is approximately half the spin-resolved level spacing.

In conclusion, we have shown that the B dependence of the conductance peaks of a Coulomb island in the quantum Hall regime are determined by the B dependence of the single-particle energy levels. The amplitude of the N th peak reflects the coupling of the N th single-particle state to the leads. The position of the N th conductance peak reflects the energy of the N th state. The Coulomb part of the energy spacing between peaks can be subtracted to obtain the single-particle energy spectrum. These measurements show the importance of the

single-particle energy states to transport in Coulomb islands and also demonstrate a powerful new tool for probing the quantized energy levels of these structures.

We wish to thank P. A. Lee, K. K. Likharev, and R. G. Wheeler for useful discussions. In addition, we thank N. R. Belk for help with the instrumentation. This work was supported by NSF Grant. No. ECS-8813250 and by the U.S. Joint Services Electronics Program under Contract No. DAAL03-89-C-001. One of us (Y.M.) acknowledges the support of a Weizmann Fellowship.

^(a)Present address: Department of Nuclear Physics, Weizmann Institute of Science, Rehovot 76100, Israel.

¹For a review of Coulomb-blockade phenomena in metals, see D. V. Averin and K. K. Likharev, in *Mesoscopic Phenomena in Solids*, edited by B. L. Altshuler, P. A. Lee, and R. A. Webb (Elsevier, Amsterdam, 1991).

²For a review of quantum transport in semiconductor nanostructures, see C. W. J. Beenakker and H. van Houten, *Solid State Phys.* **44**, 1 (1991).

³U. Meirav, M. A. Kastner, and S. J. Wind, *Phys. Rev. Lett.* **65**, 771 (1990).

⁴L. I. Glazman and R. I. Shekhter, *J. Phys. Condens. Matter* **1**, 5811 (1989); H. van Houten and C. W. J. Beenakker, *Phys. Rev. Lett.* **63**, 1893 (1989).

⁵T. P. Smith, III, *et al.*, *Phys. Rev. B* **38**, 2172 (1988); W. Hansen *et al.*, *Phys. Rev. Lett.* **62**, 2168 (1989); Ch. Sikorski and U. Merkt, *Phys. Rev. Lett.* **62**, 2164 (1989).

⁶M. A. Reed *et al.*, *Phys. Rev. Lett.* **60**, 535 (1988); C. G. Smith *et al.*, *J. Phys. C* **21**, L893 (1988).

⁷B. J. van Wees *et al.*, *Phys. Rev. Lett.* **62**, 2523 (1989).

⁸L. I. Glazman and K. A. Matveev, *Pis'ma Zh. Eksp. Teor. Phys.* **51**, 425 (1990) [*JETP Lett.* **51**, 484 (1990)].

⁹D. V. Averin and Yu. V. Nazarov, *Phys. Rev. Lett.* **65**, 2446 (1990).

¹⁰C. W. J. Beenakker, H. van Houten, and A. A. M. Staring (to be published); C. W. J. Beenakker (to be published).

¹¹Y. Meir, N. S. Wingreen, and P. A. Lee (to be published).

¹²V. Fock, *Z. Phys.* **47**, 446 (1928); C. G. Darwin, *Proc. Cambridge Philos. Soc.* **27**, 86 (1930); R. B. Dingle, *Proc. Roy. Soc. London A* **216**, 118 (1953); **219**, 463 (1953).

¹³U. Sivan and Y. Imry, *Phys. Rev. Lett.* **61**, 1001 (1988).

¹⁴U. Meirav, M. Heiblum, and Frank Stern, *Appl. Phys. Lett.* **52**, 1268 (1988).

¹⁵In all of the experiments reported here, the voltage on the upper gate is held fixed at -0.3 V.

¹⁶The inferred value of α is smaller than expected from the known upper-gate and lower-gate capacitances (see Ref. 3). The origin of this discrepancy is not known.

¹⁷See, e.g., T. Ando, A. B. Fowler, and F. Stern, *Rev. Mod. Phys.* **54**, 437 (1982).

¹⁸B. J. van Wees *et al.*, *Phys. Rev. Lett.* **62**, 1181 (1989).

¹⁹At finite temperatures the energy of a state in the second LL is only indirectly related to the position of the peak since conduction is mostly by thermal activation to states in the first LL [see Fig. 3(d)].

²⁰The remaining minor discrepancies with experiment in Fig. 3 can be accounted for within the theory by including additional single-particle states and small variations in the elastic widths.